Experimental investigation on the threshold saturation degree for the liquefaction potential of unsaturated soil

Youssef Shamas [1,2]

[1] *INSA Rouen Normandie, Normandie Univ, LMN UR 3828, F-76000, Rouen, France*

[2] *Normandie Université, UNIHAVRE, Laboratoire Ondes et Milieux Complexes, CNRS UMR 6294, Le Havre, France*

RESUME La liquéfaction est un phénomène dangereux observé principalement dans les sols sans cohésion, est bien documentée dans des conditions de pleine saturation. Cette étude explore le potentiel de liquéfaction du matériau de sable Hostun RF sous chargement dynamique dans un appareil triaxial. L'objectif de cette étude se concentre sur l'analyse du potentiel de liquéfaction du matériau de sable Hostun RF sous chargement dynamique dans un appareil triaxial. Trois tests, avec une contrainte effective initiale de 100 kPa, examinent l'influence de la densité du sol et du degré de saturation sur le potentiel de liquéfaction. Le premier test, présentant une densité relative de 71% et un degré de saturation de 96%, représente un échantillon relativement dense. Le deuxième test, avec une densité relative initiale de 55% et un degré de saturation de 85%, montre une liquéfaction sous des charges dynamiques contrôlées par la déformation dans des conditions non drainées. En revanche, le troisième test explore un échantillon peu saturé avec une densité relative de 55% et un degré de saturation initial de 62%, ne révélant aucune potentialité de liquéfaction même après 50 cycles de charge appliquée. Ces résultats suggèrent l'existence d'un seuil de degré de saturation pour la liquéfaction du sable, influencé à la fois par la densité relative initiale.

Mots-clefs Liquéfaction, Sol Non-Saturé, Sable Hostun RF, Essai Triaxial Dynamique

I. INTRODUCTION

Liquefaction is a dangerous phenomenon occurring mainly in cohesionless soils. Studies has shown the existence of liquefaction in fully saturated soils. When the pores between the soil particles is fully saturated, under specific loading, liquefaction may commence. When a static or dynamic load is exerted rapidly on the saturated soil, the water in the pores handles the exerted pressure (Seed, Arango and Chan, 1975). This causes the increase in the pore water pressure, leading to increase in pressure applied on the soil particles and push them apart from each other. This leads to the loss in the connection between the soil particles, which start to act as a liquid having no resistance to loading. In other words, during liquefaction, particularly in loose sands, soil particles tend to compress under loading, causing an increase in pore water pressure to match the total pressure. This rapid increase in pore pressure cancels the soil's effective stress, transforming it into a liquid-like state. Real life examples of earthquakes causing liquefaction have

been investigated specifying its enormous danger in inducing damage to roads and buildings due to settlements and tilting (Onoue *et al.*, 2011; Tokimatsu *et al.*, 2019; Report and Borders, 2024).

Various factors such as soil density, depth underground, and saturation degree play a critical role in determining whether liquefaction will take place or not. Previously, studies have shown that liquefaction is related exclusively to fully saturated soils. The uncertainties in numerically simulating the static liquefaction potential of saturated soils are highlighted by Huang et al (Huang *et al.*, 2024). However, recent studies have demonstrated that liquefaction may also occur in unsaturated soils (Takeshi, 1977; Vernay *et al.*, 2015), depending on various and undetermined parameters. Several studies have focused on the liquefaction potential of unsaturated soils, studying different properties such as residual soil strength post-liquefaction (Tran *et al.*, 2022a, 2023), and investigating the impact of saturation degree on the behavior of the sand in a dense state on its liquefaction potential (Tran *et al.*, 2022b).

This study focuses on analyzing different parameters in order to better understand the liquefaction potential of Hostun sand RF material under dynamic loading in a triaxial apparatus. To evaluate the influence of soil density and saturation degree on liquefaction potential, three tests were conducted with an initial effective stress of 100 kPa. The first test involved a relatively dense sample with a relative density of 71% and a saturation degree of 96%. The second test, with an initial relative density of 55% and a saturation degree of 85%, showed liquefaction under strain-controlled dynamic loads in undrained conditions. Wherever, the third test explored an unsaturated sample with an initial saturation degree of 62% and a relative density of 55%, which showed no liquefaction potential even after 50 cycles of applied load. These results suggest that there is a threshold saturation degree for sand liquefaction, influenced by both initial relative density and isotropic consolidation. Moreover, they have significant implications for the understanding and prevention of soil liquefaction in various geotechnical contexts.

II. Materials and Methods

A. Hostun Sand RF

Hostun RF sand is used as a testing reference material in France for analyzing geotechnical properties and specially liquefaction phenomena (Pan, Yang and Cai, 2020). This sand is characterized by clear fine quartz and a uniform grain distribution. Its distribution is found in the liquefiable zone of soils as defined in the literature for the potentially liquefiable soils by Iwaski (Iwasaki, 1986) (FIGURE 1). Hostun sand is well recognized for its grain-specific weight of 26.2 kN/m3, with a minimum void ratio of 0.648 and a maximum of 1.061 and a friction angle of 40° (TABLE 1). This sand has 10% of its particles with a diameter smaller than 200µm (D_{10}) and 60% of them with a diameter smaller than 400µm (D_{60}) Further information on Hostun RF sand is listed by (Amat, 2007; Goudarzy, König and Schanz, 2018).

TABLE 1. Specifications of Hostun RF Sand

Grain specific weight (kN/m³)	emax	emin	D_{10} (µm)	D_{60} (µm)	Friction angle (°)
26.2	1.061	0.648	200	400	40

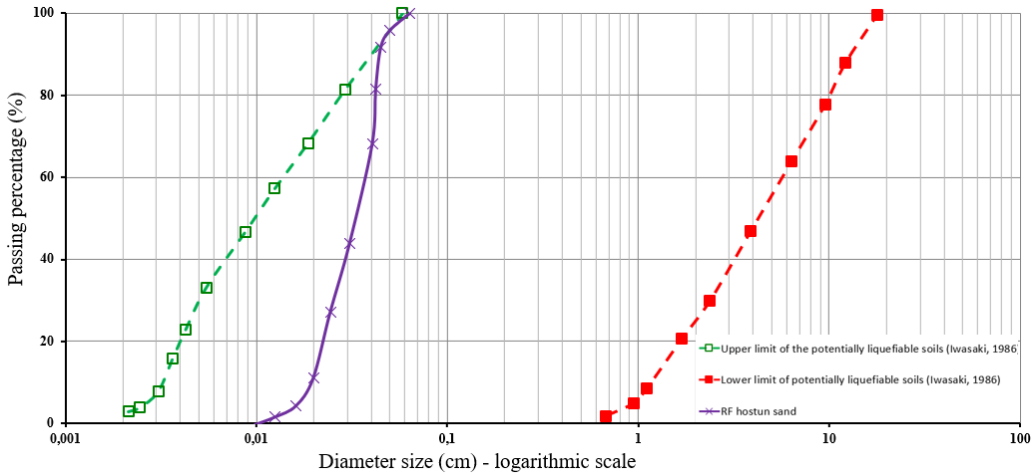

FIGURE 1. Particle Size Distribution of Hostun Sand RF in the potentially Liquefiable Domain (Iwasaki 1986)

B. Sample Preparation

Three different methods are frequently used for reconstructing soil samples in the literature: wet tamping, dry deposition, and water sedimentation. (Amini and Qi, 2000) has found no significant difference in the resistance to liquefaction between soil prepared using wet tamping and sedimentation methods. In this study, wet damping method is employed for its capability to achieve a wide range of relative densities for soil samples. The reconstituted samples are prepared using dried sand with a specific quantity of water to create a mixture with an initial water content of 8%. Then, the mixture is divided into 5 equal layers by mass and compacted layer by layer in a latex membrane placed inside a mold. The layers are compacted evenly to reach a final specimen of 70mm diameter and 140mm of height controlling the needed relative density.

The sample is reconstructed on the triaxial cell base, with filter paper and a porous stone positioned at both the bottom and top. A top cap is then placed on top of the sample to ensure the proper water drainage system, facilitating flow from the bottom of the sample towards the top.

A flexible latex membrane is used to maintain the sample and to prevent direct contact between the sample and the applied water simulating the confining pressure.

All the steps followed during the sample preparation phase are stated in the FIGURE 2.

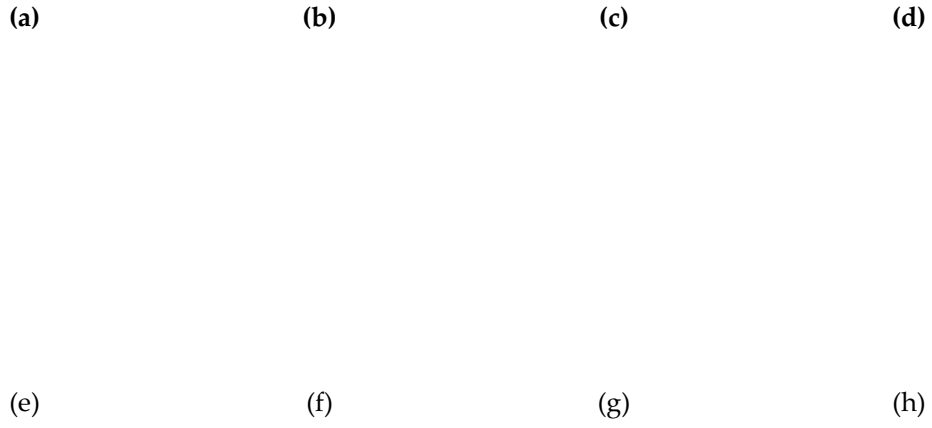

FIGURE 2. **Steps for sample preparation**

a- Dry sand. b- Mixture of sand and water. c- Division of the mixture into five equal parts. d- First compacted layer. e- Fifth and final compacted layer. f- Sample inside latex membrane with filter paper, porous stone and filter paper on the bottom and top of the sample. g- horizontality verification of the sample. h- Placing the cell and the axial transducer.

C. Dynamic Triaxial Apparatus

Dynamic Triaxial apparatus is used to simulate the application of an earthquake in soils. The earthquake waves typically have an impact on wide area, preventing water from draining quickly even in sandy soils with good permeability. One approach to replicate these circumstances involves subjecting the sample to cyclic loading in the undrained condition within a triaxial cell.

In order to replicate the actual soil conditions in the underground, the confining pressure experienced by soil at different depths underground is simulated by applying a pressure on the sample using water. An elastic latex membrane is employed to prevent direct contact between the sample and the water responsible for applying the confining pressure. The confining pressure is controlled by a Pneumatic Automatic Pressure Controller (PAPC). Additionally, the sample's saturation degree is monitored and regulated using a Hydraulic Automatic Pressure Controller (HAPC). This latter is used for applying the back pressure on the sample and recording the water volume changes. This back pressure is applied from both ends of the sample, and the pore water pressure is measured at the bottom using another transducer. Shamas et al. (Shamas *et al.*, 2024) have documented and analyzed the uncertainties associated with these experimental apparatuses.

III. Test Procedure

The initial step involves achieving the necessary initial saturation degree for the sample. This is done by flowing de-aired water from the bottom to the top of the sample, while applying a small cell pressure around it to maintain a constant effective stress. This process effectively removes most of the large air bubbles from the sample. Subsequently, a simultaneous increase in both back and cell pressure is applied until a specific volume change in water is reached corresponding to the volume change in the air inside the sample. This ensures having the required saturation degree, which is confirmed through a B-check that examines the measured change in pore pressure relative to a given change in cell pressure.

Next, the sample undergoes consolidation by maintaining the reached back pressure and increasing the cell pressure to establish a difference of 100 kPa between the applied pore pressure and cell pressure. When a stable volume change is reached, an undrained dynamic test is done on the sample under strain-controlled conditions. Seed and Idriss (SEED, H. B., & IDRISS, 1982) observed that the predominant direction of wave propagation is in the vertical orientation. In this study, a dynamic axial load is imposed on the sample by controlling a dynamic axial strain on the sample. The double amplitude of this applied strain starts with 2% as constant for 10 consecutive cycles with a frequency of 0.0125Hz or 0.00625Hz. However, if the sample is not liquefied, the double amplitude of the strain is increased to 3% for ten consecutive cycles. Same goes after that for 4% and then for the double amplitude (DA) of 5%. The latter is applied until reaching an asymptote in pore pressure change (Figure 3). A silicone funnel is used on top of the sample to apply suction between the piston and the sample, combining them together during the dynamic test. Hence this combination allows the application of the double amplitude with compressive and tensile axial strain, without affecting the sample itself.

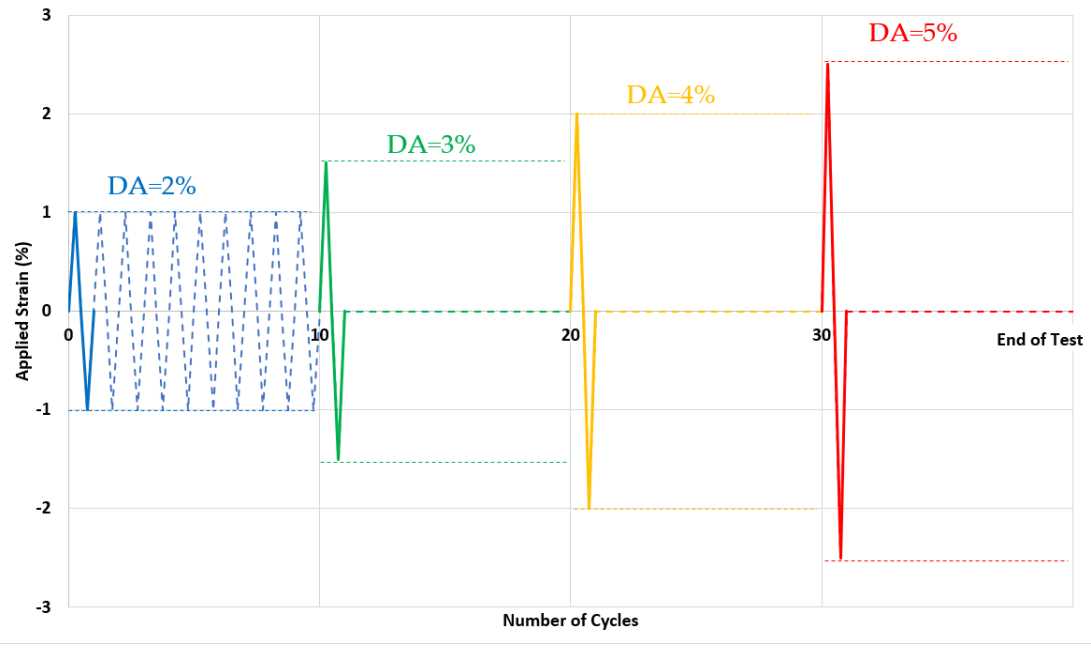

FIGURE 3. **Strain-controlled cyclic loading**

Following this liquefaction test, the sample is reconsolidated by removing the excess pore water pressure accumulated during the applied loading. Finally, a second ramp is done where the sample attains a fully saturated state. The full saturation is verified by a second B-check with a B-value exceeding 0.95 (Chaney, 1978). The sample is then removed, and its final state is determined from the calculated water content (FIGURE 4). The state of the sample and its saturation degree in each phase is confirmed using these final data combined with the recorded volume change in the pressure controllers.

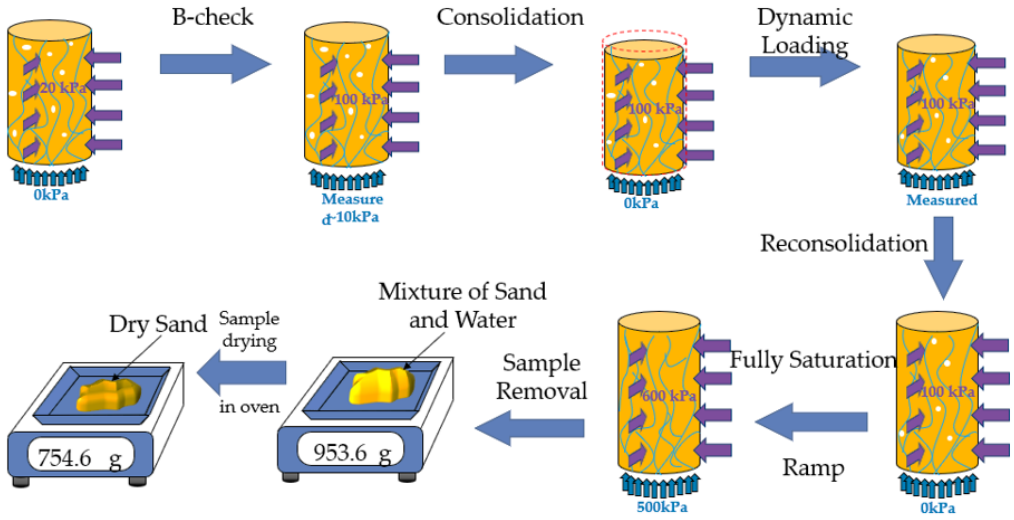

FIGURE 4. **All steps followed during the test**

For a sample with an initial saturation degree of 60%, a different technique is followed. This sample is directly placed in the triaxial test using the wet damping method, ensuring its required initial saturation degree. Consequently, the test starts directly from the third step in the previous listed phases, which is the B-check. Subsequently, all other steps follow the same procedure.

IV. Results and Discussion

A test is considered to be liquefied when the pore pressure is increased to reach the applied confining pressure. In other words, when the effective stress reaches zero, the sample is in liquefaction state.

It's significant that in specific tests, where only a 2% double amplitude is applied, the sample liquefies in less than 10 cycles. On the other hand, some tests require more cycles, reaching a 4% in double amplitude of applied strain, a total of 27 cycles are needed to reach the liquefaction. However, there is a case where a sample, despite reaching a 5% amplitude in applied strain corresponding to 17 cycles under this applied strain (or 47 cycles from the beginning of the loading phase), does not show any liquefaction potential.

Two tests with different initial relative densities exhibit liquefaction. Whereas, one test with a 56% relative density, before the dynamic load, and a low initial saturation degree does not present any liquefaction behavior. The summarized results of the tests are presented in TABLE 2.

TABLE 2. Summary of the performed tests

Test Number	Initial Void ratio	Initial relative density (%)	Initial saturation degree (%)	Number of applied cycles	Test Result
1	0.83	55	85	27	Liquefaction
2	0.82	56	62	47	No Liquefaction
3	0.76	71	96	7	Liquefaction

The sample in test 3 with an initial relative density of 71% reaches liquefaction rapidly, at the seventh cycle, with only using the strain load of a double amplitude of 2%. The saturation degree for this specimen, recorded before the undrained test, is 97.8% (after the consolidation step and before loading phase). Despite being highly saturated but not fully saturated, this condition facilitates the liquefaction of the sample. Additionally, in the liquefied state, the sample's strength decreases rapidly to reach zero (FIGURE 5). This is related to the rapid increase in the pore water pressure, reaching the initial effective stress as depicted in FIGURE 6. All this leads to liquefaction where the soil particles lose their connections. The decrease in the deviatoric stress with respect to the change in the mean effective stress is shown in FIGURE 7. This shows that the initial slope between the deviatoric stress and the mean effective stress has a ratio of 1 to 3 (in path from point a to b in FIGURE 7).

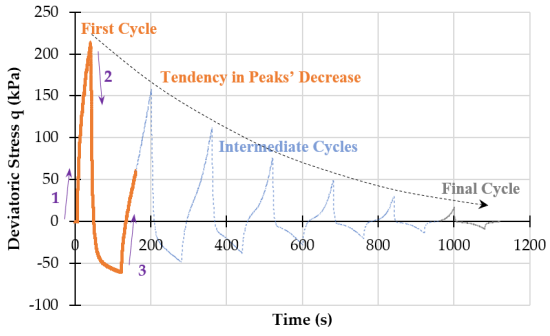

FIGURE 5. **Decrease in deviatoric stress along time**

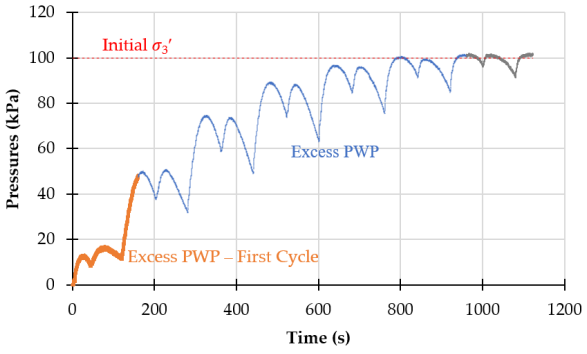

FIGURE 6. **Evolution of the Pore Water Pressure to reach the initial effective stress**

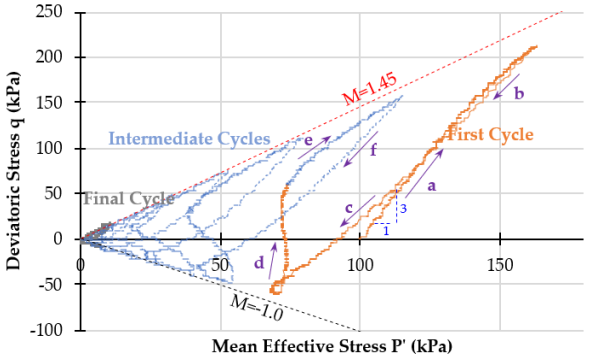

FIGURE 7. **Deviatoric stress vs mean effective stress**

The second test (Test 2) shows no liquefaction and all the results are presented in FIGURES 8, 9 and 10. The sample has a relative density of 55% and an initial saturation degree of 62% before the undrained test. The test is stopped after a total of 47 cycles (from the beginning of the loading phases), corresponding to 17 cycles under the strain loading of a double amplitude of 5%. FIGURE 8 presents the change in the deviatoric stress with respect to the applied strain with double amplitudes of 2%, 3%, 4%, and 5%, showing the first cycle in each loading step. There is no obvious decrease in the maximum deviatoric stress reached in each loading phase. There is only a slight decrease in the modulus of the sample. The initial stress applied was 100 kPa, while the pore pressure slightly increases, reaching only 12 kPa and stabilizing at this level (FIGURE 9). FIGURE 10 shows clearly the evolution of the pore pressure from 0 to 12 kPa.

FIGURE 8. **Decrease in deviatoric stress along time**

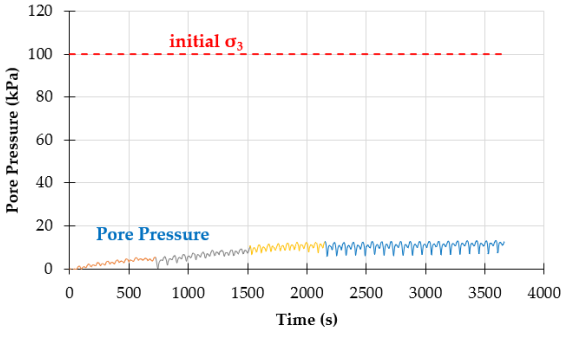

FIGURE 9. **Pore pressure change with time**

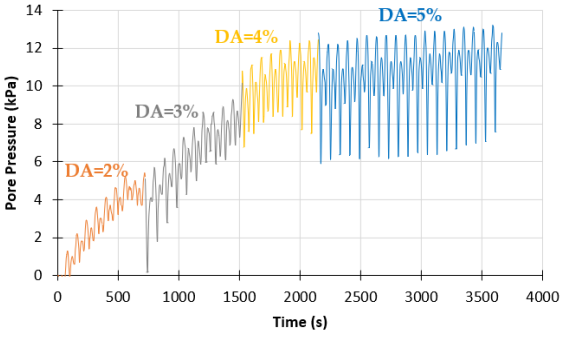

FIGURE 10. **Zoom-in to the pressure change zone**

V. Conclusion

Several experiments are conducted on reconstituted Hostun RF sand to study liquefaction potential in unsaturated soil, based on specific parameters. The results highlight the critical influence of saturation degree in preventing liquefaction; whereas, unsaturated samples can liquefy under specific conditions. Additionally, relative density emerges as a contributing factor to the material's liquefaction potential. Further research is needed to precisely define the thresholds of these influencing parameters to avoid liquefaction. Furthermore, a comprehensive examination of various parameters simultaneously is essential for discovering their connections and understanding how they influence the liquefaction phenomenon.

This study verifies the existence of liquefaction potential in the unsaturated soils. Moreover, it demonstrates the evolution of the pore pressure during the undrained test to reach liquefaction.

Finally, this study shows that there is a threshold related to many factors, including the saturation degree and relative density, to liquefy or not the soil.

REFERENCES

Amat, A.S. (2007) 'Elastic Stiffness Moduli of Hostun Sand', *University of Bristol*, (June), pp. 1–61.

Amini, F. and Qi, G.Z. (2000) 'L Iquefaction T Esting of', *Manager*, 126(March), pp. 208–217.

Chaney, R.C. (1978) 'Saturation Effects on the Cyclic Strength of Sands', in. Available at: https://api.semanticscholar.org/CorpusID:137553265.

Goudarzy, M., König, D. and Schanz, T. (2018) 'Interpretation of small and intermediate strain characteristics of Hostun sand for various stress states', *Soils and Foundations*, 58(6), pp. 1526–1537. Available at: https://doi.org/10.1016/j.sandf.2018.09.002.

Huang, W.H. *et al.* (2024) 'Uncertainties of Numerical Simulation for Static Liquefaction Potential of Saturated Soils BT - Proceedings of the 6th International Symposium on Uncertainty Quantification and Stochastic Modelling', in J.E.S. De Cursi (ed.). Cham: Springer International Publishing, pp. 1–15.

Iwasaki, T. (1986) 'Soil liquefaction studies in Japan: state-of-the-art', *Soil Dynamics and Earthquake Engineering*, 5(1), pp. 2–68. Available at: https://doi.org/10.1016/0267-7261(86)90024-2.

Onoue, A. *et al.* (2011) 'Review of topographic and soil conditions for liquefaction-related damage induced by the 2007 off Mid-Niigata Earthquake', *Soils and Foundations*, 51(3), pp. 533–548. Available at: https://doi.org/10.3208/sandf.51.533.

Pan, K., Yang, Z.X. and Cai, Y.Q. (2020) 'Flow liquefaction potential of loose sand: stress path envelope and energy-based evaluation', *Canadian Geotechnical Journal*, 58(11), pp. 1783–1789. Available at: https://doi.org/10.1139/cgj-2019-0366.

Report, F.P. and Borders, G.W. (2024) 'Noto Hanto (=Peninsula) Earthquake January 1', 6. Available at: https://www.google.com/url?sa=t&rct=j&q=&esrc=s&source=web&cd=&ved=2ahUKEwif1_Cl7OeFAxXZRaQEHY-VBCsQFnoECDAQAQ&url=http%3A%2F%2Fwww.hssmge.gr%2FNoto%2520HANTO%25202024%2520Ground%2520Motions.pdf&usg=AOvVaw3KLlNrqJzIl4zAWJFw1vUt&opi=89978449.

SEED, H. B., & IDRISS, I.M. (1982) 'Ground motions and soil liquefaction during earthquakes.', *IEEE Industry Applications Magazine*, 13(2), pp. 78–79. Available at: https://doi.org/10.1109/MIA.2007.322261.

Seed, H.B., Arango, I. and Chan, C.K. (1975) 'Evaluation of soil liquefaction potential for level ground during earthquakes: A summary report', p. 113. Available at: http://www.osti.gov/servlets/purl/7146067.

Shamas, Y. *et al.* (2024) 'Uncertainties of Experimental Tests on Cyclic Liquefaction Potential of Unsaturated Soils BT - Proceedings of the 6th International Symposium on Uncertainty Quantification and Stochastic Modelling', in J.E.S. De Cursi (ed.). Cham: Springer International Publishing, pp. 30–41.

Takeshi, N. (1977) 'NII-Electronic Library Service', *Chemical Pharmaceutical Bulletin*, 57(534), pp.

364–370. Available at: http://www.mendeley.com/research/geology-volcanic-history-eruptive-style-yakedake-volcano-group-central-japan/.

Tokimatsu, K. *et al.* (2019) 'Liquefaction-induced settlement and tilting of buildings with shallow foundations based on field and laboratory observation', *Soil Dynamics and Earthquake Engineering*, 124(May 2018), pp. 268–279. Available at: https://doi.org/10.1016/j.soildyn.2018.04.054.

Tran, K.-H. *et al.* (2022a) 'Effect of saturation on liquefaction potential and residual strength: laboratory investigation', *European Journal of Environmental and Civil Engineering*, 26(15), pp. 7480–7502. Available at: https://doi.org/10.1080/19648189.2021.1999333.

Tran, K.-H. *et al.* (2022b) 'Investigation of the influence of saturation degree on the cyclic behaviour of fine clear sand', *Academic Journal of Civil Engineering*, 40(1), pp. 66–70. Available at: https://doi.org/10.26168/ajce.40.1.17.

Tran, K.-H. *et al.* (2023) 'Liquefaction of unsaturated soils- volume change and residual shear strength', *European Journal of Environmental and Civil Engineering*, 27(3), pp. 1144–1164. Available at: https://doi.org/10.1080/19648189.2022.2075471.

Vernay, M. *et al.* (2015) 'Etude du comportement des sols non satur ´ es ` a la efaction To cite this version : Etude du comportement des sols non saturés à la liquéfaction'. Available at: https://hal.archives-ouvertes.fr/hal-01167662.